

Atlantic overturning responses to Late Pleistocene climate forcings

Lorraine E. Lisiecki¹†, Maureen E. Raymo¹ & William B. Curry²

The factors driving glacial changes in ocean overturning circulation are not well understood. On the basis of a comparison of 20 climate variables over the past four glacial cycles, the SPECMAP project¹ proposed that summer insolation at high northern latitudes (that is, Milankovitch forcing) drives the same sequence of ocean circulation and other climate responses over 100-kyr eccentricity cycles, 41-kyr obliquity cycles and 23-kyr precession cycles. SPECMAP analysed the circulation response at only a few sites in the Atlantic Ocean, however, and the phase of circulation response has been shown to vary by site and orbital band². Here we test the SPECMAP hypothesis by measuring the phase of orbital responses in benthic $\delta^{13}\text{C}$ (a proxy indicator of ocean nutrient content) at 24 sites throughout the Atlantic over the past 425 kyr. On the basis of $\delta^{13}\text{C}$ responses at 3,000–4,010 m water depth, we find that maxima in Milankovitch forcing are associated with greater mid-depth overturning in the obliquity band but less overturning in the precession band. This suggests that Atlantic overturning is strongly sensitive to factors beyond ice volume and summer insolation at high northern latitudes. A better understanding of these processes could lead to improvements in model estimates of overturning rates, which range from a 40 per cent increase to a 40 per cent decrease at the Last Glacial Maximum³ and a 10–50 per cent decrease over the next 140 yr in response to projected increases in atmospheric CO_2 (ref. 4).

Different modes of Atlantic overturning appear to be coupled with widespread climate change on both orbital^{1,5,6} and millennial^{7,8} time-scales. Today, North Atlantic Deep Water (NADW) fills most of the Atlantic at 2,000–4,000 m water depth, above deep water of Southern Ocean origin. During the Last Glacial Maximum (LGM), nutrient-poor NADW shoaled to less than 2,000 m and was replaced by nutrient-rich Southern Ocean Water (SOW), according to Atlantic transects of the $\delta^{13}\text{C}$ and Cd/Ca ratio of LGM benthic foraminifera^{9,10}. Although these two proxies can be influenced by several biogeochemical factors unrelated to ocean circulation^{9–11}, independent estimates of overturning since the LGM are consistent with these tracer changes^{7,12}. Comparisons of Pleistocene Atlantic $\delta^{13}\text{C}$ records with the ice-volume proxy benthic $\delta^{18}\text{O}$ show that the presence of NADW below 2,000 m is strongly correlated with the size of northern ice sheets^{12,13}. However, important differences between $\delta^{13}\text{C}$ and $\delta^{18}\text{O}$ suggest that ice volume is not the only factor controlling NADW circulation^{2,13}.

In the sequence of circulation responses described by SPECMAP¹, lower NADW formation, the ‘Nordic heat pump’, responds rapidly to Milankovitch forcing, and mid-depth (~3,400 m) overturning in the North Atlantic responds later, slightly lagging ice volume. (This mid-depth response is not equivalent to the ‘boreal heat pump’, which is the mechanism SPECMAP proposed for the production of Glacial North Atlantic Intermediate Water (GNAIW)⁶.) We analyse benthic $\delta^{13}\text{C}$ records of the past 425 kyr from 24 Atlantic sites and 5

Pacific sites (Supplementary Table 1 and Supplementary Fig. 1) to evaluate the SPECMAP hypothesis that circulation response has the same phase relative to ice volume in all three orbital bands. We focus on mid-depth sites because circulation responses at these sites are more easily distinguished from changes in the $\delta^{13}\text{C}$ composition of NADW and SOW.

We place all benthic $\delta^{13}\text{C}$ records on the same age model¹⁴ (Methods) and calculate $\Delta\delta^{13}\text{C}$ by taking the difference between each Atlantic $\delta^{13}\text{C}$ record and a record of mean ocean $\delta^{13}\text{C}$, estimated by averaging five Pacific $\delta^{13}\text{C}$ records (Fig. 1). Figure 2 shows the phase of $\Delta\delta^{13}\text{C}$ at each site relative to obliquity and precession (June perihelion). (See Supplementary Information for eccentricity phases.) Also shown is the phase of benthic $\delta^{18}\text{O}$ (times -1), which we refer to as minimum ice volume for simplicity but which also contains a significant deep water temperature component (Supplementary Information).

The orbital phases of Atlantic $\Delta\delta^{13}\text{C}$ can be well described by dividing the sites into three groups according to water depth. On the basis of modern and LGM $\delta^{13}\text{C}$ transects⁹, we interpret the $\Delta\delta^{13}\text{C}$ of sites at 1,100–2,301 m depth as primarily recording the $\delta^{13}\text{C}$ composition of NADW, sites from 3,000 to 4,010 m as primarily recording changes in the mixing ratio of NADW and SOW, and sites from 4,035 to 4,620 m as primarily recording the $\delta^{13}\text{C}$ of SOW. The consistency of phase relationships within these depth intervals, despite a wide range of latitude and longitude, strongly suggests that these responses are basin-wide and that the $\delta^{13}\text{C}$ of deep water is accurately recorded.

At all three frequencies, most sites above 2,300 m have large phase lags (140° – 260°), consistent with increases in GNAIW and the $\Delta\delta^{13}\text{C}$ of upper NADW during glacial conditions^{6,9}. However, at most sites from 3,000 to 4,010 m, $\Delta\delta^{13}\text{C}$ leads minimum ice volume in the obliquity band but lags it in the precession band. Mid-depth lags relative to Milankovitch forcing, which we define to be 21 June insolation at 65°N (Supplementary Information), are 3° – 26° (0–3 kyr) in the obliquity band and 100° – 176° (6–11 kyr) in the precession band. This represents a significant challenge to the SPECMAP hypothesis that circulation responds with the same phase in all orbital bands¹. Evidence that benthic $\delta^{18}\text{O}$ change can differ from ice volume change by 2.2 kyr (ref. 15) cannot account for the ~6-kyr shift in $\delta^{13}\text{C}$ phase between the obliquity and precession bands.

The difference between obliquity and precession responses was not observed by SPECMAP because they analysed mid-depth $\delta^{13}\text{C}$ only at ODP site 607 (ref. 16), which has atypical obliquity and precession phases in comparison with most other mid-depth sites. However, our results are consistent with previously reported phases at several western equatorial Atlantic sites². Mid-depth sites in the Atlantic western boundary current (squares in Fig. 2) tend to have strong precession and obliquity power and large precession lags. Eastern Atlantic sites

¹Department of Earth Sciences, Boston University, 675 Commonwealth Avenue, Boston, Massachusetts 02215, USA. ²Department of Geology and Geophysics, Woods Hole Oceanographic Institution, Woods Hole, Massachusetts 02543, USA. †Present address: Department of Earth Science, University of California, Santa Barbara, Santa Barbara, California 93106-9630, USA.

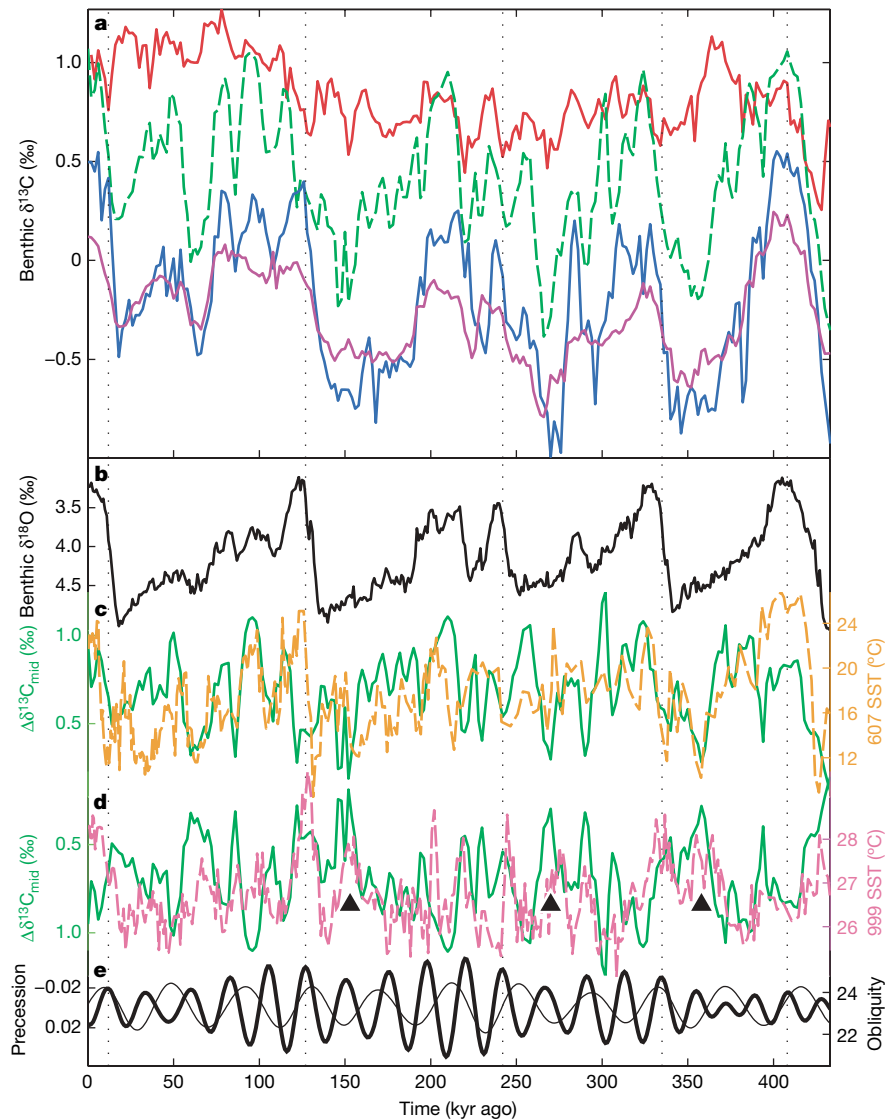


Figure 1 | Comparison of benthic $\delta^{13}\text{C}$, orbital forcing, ice volume and SST. **a**, Regional stacks (averages) of benthic $\delta^{13}\text{C}$ (‰ VPDB) from shallow North Atlantic sites (red; mean from sites DSDP552, ODP980, ODP982, ODP983), selected mid-depth Atlantic sites (green dashed; ODP925, ODP927, ODP928, GeoB1214), deep Atlantic sites (blue; ODP929, ODP1089, GeoB1041, GeoB1211), and Pacific sites (purple; ODP677, ODP846,

ODP849, RC13-110, V21-146). **b**, Benthic $\delta^{18}\text{O}$ (‰ VPDB; black, ref. 14) as a proxy for ice volume. **c**, North Atlantic summer SST¹⁹ ('607 SST', orange) and $\Delta\delta^{13}\text{C}_{\text{mid}}$ (green, $\delta^{13}\text{C}_{\text{mid}} - \delta^{13}\text{C}_{\text{Pac}}$). **d**, Caribbean SST²¹ ('999 SST', pink) and $\Delta\delta^{13}\text{C}_{\text{mid}}$ (green, y-axis reversed). Triangles mark SST peaks preceding glacial maxima. **e**, Precession index (thick) and obliquity (thin), plotted such that greater Milankovitch forcing is up.

with less precession power and smaller precession lags could be less sensitive to circulation change because they are farther from the main path for meridional deep water transport.

To investigate the differences between precession and obliquity responses, we calculate $\Delta\delta^{13}\text{C}_{\text{mid}}$ by averaging the four mid-depth sites with the greatest precession lags (Fig. 1c). $\Delta\delta^{13}\text{C}_{\text{mid}}$ displays significantly different phases with respect to ice volume in the obliquity and precession bands (Fig. 3). In the obliquity band, $\Delta\delta^{13}\text{C}_{\text{mid}}$ is nearly in phase with Milankovitch forcing, suggesting a rapid response to obliquity-driven insolation change. In the precession band, $\Delta\delta^{13}\text{C}_{\text{mid}}$ is not easily interpreted as a response to Milankovitch forcing or ice volume because it lags June perihelion by 170° (11 kyr) and minimum ice volume by 100° (6.4 kyr). Because circulation is unlikely to lag its forcing by more than 90° , we discuss the alternative possibility that the insolation forcing at June perihelion produces a minimum in $\Delta\delta^{13}\text{C}_{\text{mid}}$ with very little lag.

Is the minimum in $\Delta\delta^{13}\text{C}_{\text{mid}}$ at June perihelion caused by a change in circulation? Mid-depth $\Delta\delta^{13}\text{C}$ is affected by the mixing ratio of NADW and SOW and by the $\delta^{13}\text{C}$ composition of each water mass. However, the $\delta^{13}\text{C}$ of NADW as recorded by shallow North Atlantic

sites has much less precession power than $\Delta\delta^{13}\text{C}_{\text{mid}}$ (Supplementary Fig. 2), and the $\Delta\delta^{13}\text{C}$ of SOW as recorded by deep South Atlantic sites has a significantly different phase from $\Delta\delta^{13}\text{C}_{\text{mid}}$ (Fig. 3b). Therefore, the minimum in $\Delta\delta^{13}\text{C}_{\text{mid}}$ at June perihelion must primarily reflect a reduction in the mixing ratio of NADW at these sites, probably due to weaker and/or shallower North Atlantic overturning.

Although $\delta^{13}\text{C}$ gradients cannot unequivocally constrain the rate of meridional overturning¹⁷, changes in meridional heat transport, inferred from Atlantic sea surface temperature (SST) records, may provide indirect evidence for changes in overturning rate⁸. For example, during stadial events of the last glacial cycle, reduced overturning is associated with cooling at high northern latitudes⁷ and warming at low latitudes^{8,18}, consistent with a decrease in meridional heat transport. If $\Delta\delta^{13}\text{C}_{\text{mid}}$ records orbitally driven changes in overturning rate, we expect $\Delta\delta^{13}\text{C}_{\text{mid}}$ to be in phase with North Atlantic SST and antiphased with low-latitude SST (Supplementary Information).

In the precession band, we find that SST estimates based on foraminiferal species counts at ODP Site 607 (Fig. 1c, ref. 19) and other North Atlantic sites^{5,20} are nearly in phase with $\Delta\delta^{13}\text{C}_{\text{mid}}$ (Fig. 3d),

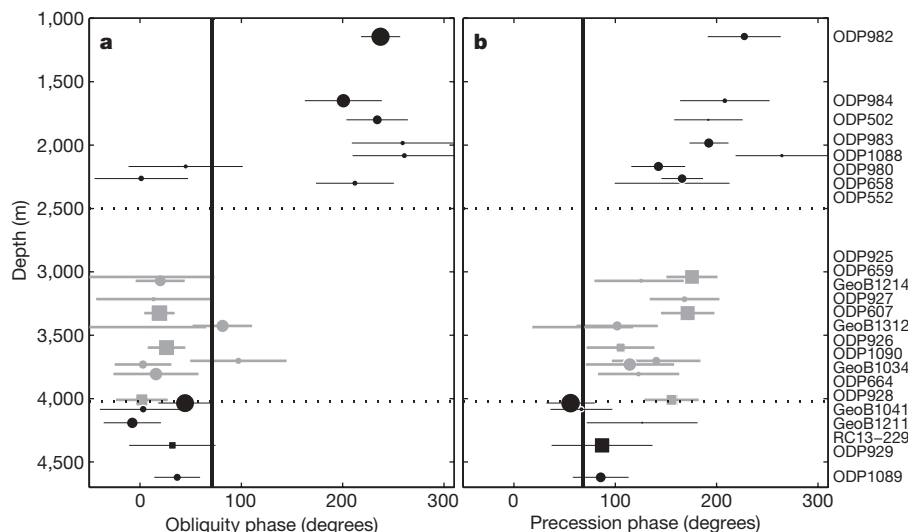


Figure 2 | Phases of orbital responses of benthic $\Delta\delta^{13}\text{C}$ in the Atlantic. Symbols mark the phase of each site, with 2σ error bars, relative to **a**, 41-kyr obliquity and **b**, 23-kyr precession (June perihelion). The vertical line in each panel marks the phase of minimum ice volume from benthic $\delta^{18}\text{O}$ (ref. 14). Squares denote western Atlantic Ceara rise sites; circles, all other sites. The

size of each symbol is proportional to the coherent amplitude of the response. Dotted lines separate different depth ranges; grey symbols denote mid-depth sites. (Site 502 at a depth of 3,051 m in the Caribbean basin is plotted at the sill depth of 1,800 m.)

consistent with a change in overturning rate and out-of-phase with local summer insolation. A Caribbean foraminiferal Mg/Ca record of SST²¹ (Fig. 1d) is antiphased with $\Delta\delta^{13}\text{C}_{\text{mid}}$ (Fig. 3d), consistent with the proposed overturning changes, but also in phase with local summer insolation forcing²¹. We suggest that the effects of overturning can be distinguished from insolation forcing during prominent SST peaks preceding glacial maxima (marked by triangles in Fig. 1d). This low-latitude warming is consistent with the reduced overturning suggested

by $\Delta\delta^{13}\text{C}_{\text{mid}}$ but difficult to explain otherwise, given relatively weak precession forcing, high ice volume and low atmospheric partial pressure of CO_2 (p_{CO_2} ; ref. 22). Therefore, Atlantic SST responses appear consistent with reduced overturning rates during June perihelion, as suggested by $\Delta\delta^{13}\text{C}_{\text{mid}}$.

In the obliquity band, the phases of Atlantic SST at both high and low latitudes are similar (Fig. 3c) rather than antiphased and, thus, provide no constraints on the phase of overturning response. The fact that both SST records are approximately in phase with ice volume and p_{CO_2} (Supplementary Table 2) suggests that these factors may overwhelm any SST signal due to obliquity-driven overturning changes. In contrast, ice volume and p_{CO_2} (ref. 22) have less power in the precession band, which may explain why the effects of overturning on SST are visible for precession but not obliquity.

Can modelling studies be used to provide another test of circulation responses to obliquity and precession? It seems not; at present, the response of North Atlantic overturning to orbital forcing or even LGM boundary conditions³ is highly model-dependent. Increasing Milankovitch forcing decreases NADW formation in some models^{23,24} and increases it in others^{25,26}. One study that varied obliquity and precession separately found that greater Milankovitch forcing from either precession or obliquity increased overturning²⁶. However, another found that greater Milankovitch forcing decreased overturning in the obliquity band but increased it in the precession band²⁷. Additionally, neither of these models included a Laurentide ice sheet. In fact, given the wide range of model results, our results may provide an important metric against which future models could be evaluated; our results could be further tested with additional SST records and other circulation proxies.

The phases of $\Delta\delta^{13}\text{C}_{\text{mid}}$ place constraints on the forcing mechanisms important for mid-depth overturning. Greater Milankovitch forcing decreases ice volume in both the obliquity and precession bands but corresponds to different $\Delta\delta^{13}\text{C}_{\text{mid}}$ responses. Therefore, mid-depth overturning must also be sensitive to factors other than Milankovitch forcing and ice volume. The different seasonal and spatial insolation anomalies associated with precession versus obliquity provide many mechanisms by which the two orbital cycles could produce different overturning responses.

The strongest insolation forcing that is antiphased with Milankovitch forcing in one orbital band but not the other occurs at high southern latitudes in summer. Weaker forcing occurs over

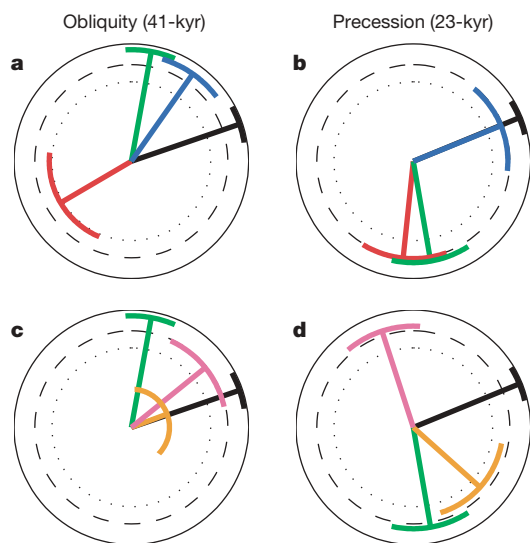


Figure 3 | Comparison of $\Delta\delta^{13}\text{C}$ and SST phases. **a**, **b**, The phases for obliquity (**a**) and precession (**b**) of minimum ice volume from benthic $\delta^{18}\text{O}$ (black, ref. 14) and regional stacks of Atlantic $\Delta\delta^{13}\text{C}$ for shallow North Atlantic sites (red), selected mid-depth sites (green) and $>4,010$ m sites (blue). **c**, **d**, The phases for obliquity (**c**) and precession (**d**) of benthic $\delta^{18}\text{O}$ (black, ref. 14), $\Delta\delta^{13}\text{C}_{\text{mid}}$ (green), North Atlantic SST¹⁹ (orange) and Caribbean SST²¹ (pink). In this phase wheel representation, vectors in the 12 o'clock position are in phase with maximum Milankovitch forcing, and phase lags increase in the clockwise direction (for example, 3 o'clock represents a 90° lag relative to Milankovitch forcing, 6 o'clock represents an antiphased response, and 9 o'clock represents a 90° lead). Vector length (from circle centre to middle of arc) represents coherence, and the associated arc denotes the 2σ phase error. Circles mark 100% (solid), 95% (dashed) and 80% (dotted) coherence.

southern mid-latitudes in summer, southern low- and mid-latitudes in winter, and high northern latitudes in late summer (Supplementary Fig. 7). Perhaps cooler southern summers during June perihelion, obliquity minima, and glacial maxima reduce mid-depth NADW by enhancing SOW formation²⁸. However, Antarctic temperature appears to be in phase with Milankovitch forcing rather than local summer insolation²⁹. Alternatively, reduced insolation in late summer at high northern latitudes³⁰ might decrease NADW formation by altering North Atlantic sea ice extent, salinity or temperature. The different phases of circulation response relative to Milankovitch forcing associated with obliquity and precession may produce different climate feedbacks, which may affect the amplitude of ice volume response at the two frequencies.

METHODS SUMMARY

The $\delta^{13}\text{C}$ records in this study are collected from previous studies (Supplementary Information) and primarily measured from the epibenthic taxon *Cibicides wuellerstorfi*. All records are placed on a common age model by aligning their benthic $\delta^{18}\text{O}$ records to the LR04 benthic $\delta^{18}\text{O}$ stack¹⁴. (Site ODP999 (ref. 21) was aligned using planktonic $\delta^{18}\text{O}$.) See ref. 14 for detailed alignment methodology.

We reconstruct circulation changes at mid-depth sites using the $\Delta\delta^{13}\text{C}$ instead of percentage NADW¹ because we wish to avoid the assumption that the $\delta^{13}\text{C}$ of SOW and NADW are consistently recorded by any of the available sites. In particular, many of our deep Atlantic (SOW) sites have a non-negligible percentage NADW today. However, the phases of percentage NADW for mid-depth sites (Supplementary Fig. 3) are not significantly different from those of $\Delta\delta^{13}\text{C}$. Additionally, the phases of $\Delta\delta^{13}\text{C}$ are not significantly different from $\delta^{13}\text{C}$ (Supplementary Fig. 4), except at several shallow Atlantic sites.

Before spectral analysis, all records are interpolated to an even 1-kyr time step from 15 to 425 kyr ago. Spectral analysis was performed with the ARAND software package (P. Howell, N. Piasis, J. Ballance, J. Baughman and L. Ochs, Brown University), which uses the Blackman–Tukey technique. Phases were calculated by cross spectral analysis with ETP (the sum of normalized eccentricity plus obliquity minus the precession index) using a maximum lag of 150 kyr. Error bars on phase estimates do not include the age model uncertainty of ~4 kyr. This uncertainty affects phases relative to Milankovitch forcing but not relative to benthic $\delta^{18}\text{O}$, and may explain why Caribbean SST and minimum $\Delta\delta^{13}\text{C}_{\text{mid}}$ appear to lead June perihelion slightly.

Received 9 January; accepted 9 September 2008.

1. Imbrie, J. *et al.* On the structure and origin of major glaciation cycles. 1. Linear responses to Milankovitch forcing. *Paleoceanography* **7**, 701–738 (1992).
2. Curry, W. B. in *The South Atlantic: Past and Present Circulation* (eds Wefer, G., Berger, W. H., Siedler, G. & Webb, D.) 577–598 (Springer, 1996).
3. Weber, S. L. *et al.* The modern and glacial overturning circulation in the Atlantic ocean in PMIP coupled model simulations. *Clim. Past* **3**, 51–64 (2007).
4. Gregory, J. M. *et al.* A model intercomparison of changes in the Atlantic thermohaline circulation in response to increasing atmospheric CO_2 concentration. *Geophys. Res. Lett.* **32**, L12703, doi:10.1029/2005GL023209 (2005).
5. McManus, J. F., Oppo, D. W., Keigwin, L. D., Cullen, J. L. & Bond, G. C. Thermohaline circulation and prolonged interglacial warmth in the North Atlantic. *Quat. Res.* **58**, 17–21 (2002).
6. Boyle, E. A. & Keigwin, L. North Atlantic thermohaline circulation during the past 20,000 years linked to high-latitude surface temperature. *Nature* **330**, 35–40 (1987).
7. McManus, J. F., Francois, R., Gherardi, J.-M., Keigwin, L. D. & Brown-Leger, S. Collapse and rapid resumption of Atlantic meridional circulation linked to deglacial climate changes. *Nature* **428**, 834–837 (2004).
8. Dahl, K. A., Broccoli, A. J. & Stouffer, D. J. Assessing the role of North Atlantic freshwater forcing in millennial scale climate variability: A tropical Atlantic perspective. *Clim. Dyn.* **24**, 325–346 (2005).
9. Curry, W. B. & Oppo, D. W. Glacial water mass geometry and the distribution of $\delta^{13}\text{C}$ of ΣCO_2 in the western Atlantic Ocean. *Paleoceanography* **20**, PA1017, doi:10.1029/2004PA001021 (2005).

10. Marchitto, T. M. & Broecker, W. S. Deep water mass geometry in the glacial Atlantic Ocean: A review of constraints from the paleonutrient proxy Cd/Ca. *Geochim. Geophys. Geosyst.* **7**, Q12003, doi:10.1029/2006GC001323 (2006).
11. Mackensen, A., Hubberton, H.-W., Bickert, T., Fischer, G. & Fütterer, D. K. The $\delta^{13}\text{C}$ in benthic foraminiferal tests of *Fontbotia Wuellerstorfi* (Schwager) relative to the $\delta^{13}\text{C}$ of dissolved inorganic carbon in Southern Ocean Deep Water: Implications for glacial ocean circulation models. *Paleoceanography* **8**, 587–610 (1993).
12. McCave, I. N., Manighetti, B. & Beveridge, N. A. S. Circulation in the glacial North Atlantic inferred from grain-size measurements. *Nature* **374**, 149–152 (1995).
13. Raymo, M. E., Ruddiman, W. F., Shackleton, N. J. & Oppo, D. W. Evolution of the Atlantic-Pacific $\delta^{13}\text{C}$ gradients over the last 2.5 m.y. *Earth Planet. Sci. Lett.* **93**, 353–368 (1990).
14. Lisiecki, L. E. & Raymo, M. E. A. Pliocene-Pleistocene stack of 57 globally distributed benthic $\delta^{18}\text{O}$ records. *Paleoceanography* **20**, PA1003, doi:10.1029/2004PA001071 (2005).
15. Skinner, L. C. & Shackleton, N. J. An Atlantic lead over Pacific deep-water change across Termination I: Implications for the application of the marine isotope stage stratigraphy. *Quat. Sci. Rev.* **24**, 571–580 (2005).
16. Ruddiman, W. F., Raymo, M. E., Martinson, D. G., Clement, B. M. & Backman, J. Pleistocene evolution: Northern hemisphere ice sheets and North Atlantic Ocean. *Paleoceanography* **4**, 353–412 (1989).
17. Huybers, P., Gebbie, G. & Marchal, O. Can paleoceanographic tracers constrain meridional circulation rates? *J. Phys. Oceanogr.* **37**, 394–407 (2007).
18. Ruhlmann, C., Mulitza, S., Muller, P. J., Wefer, G. & Zahn, R. Warming of the tropical Atlantic Ocean and slowdown of thermohaline circulation during the last deglaciation. *Nature* **402**, 511–514 (1999).
19. Ruddiman, W. F. & McIntyre, A. Oceanic mechanisms for amplification of the 23,000-year ice-volume cycle. *Science* **212**, 617–627 (1981).
20. Imbrie, J., McIntyre, A. & Mix, A. in *Climate and Geo-Sciences* (eds Berger, A. *et al.*) 121–164 (Kluwer Academic, 1989).
21. Schmidt, M. W., Vautravers, M. J. & Spero, H. J. Western Caribbean sea surface temperatures during the late Quaternary. *Geochim. Geophys. Geosyst.* **7**, Q02P10, doi:10.1029/2005GC000957 (2006).
22. Petit, J. R. *et al.* Climate and atmospheric history of the past 420,000 years from the Vostok ice core, Antarctica. *Nature* **399**, 429–436 (1999).
23. Wang, Z. & Mysak, L. A. Simulation of the last glacial inception and rapid ice sheet growth in the McGill paleoclimate model. *Geophys. Res. Lett.* **29**, doi:10.1029/2002GL015120 (2002).
24. Khodri, M. *et al.* Modelling the climate evolution from the last interglacial to the start of the last glaciation: The role of Arctic Ocean freshwater budget. *Geophys. Res. Lett.* **30**, 1606, doi:10.1029/2003GL017108 (2003).
25. Yoshimori, M., Weaver, A. J., Marshall, S. J. & Clarke, G. K. C. Glacial termination: Sensitivity to orbital and CO_2 forcing in a coupled climate system model. *Clim. Dyn.* **17**, 571–588 (2001).
26. Crucifix, M. & Loutre, M. F. Transient simulations over the last interglacial period (125–115 kyr BP): Feedback and forcing analysis. *Clim. Dyn.* **19**, 417–433 (2002).
27. Tuenter, E., Weber, S. L., Hilgen, F. J., Lourens, L. J. & Ganopolski, A. Simulation of climate phase lags in response to precession and obliquity forcing and the role of vegetation. *Clim. Dyn.* **24**, 279–295 (2005).
28. Shin, S., Liu, Z., Otto-Bliesner, B., Brady, E. & Kutzbach, J. Southern Ocean sea-ice control of the glacial North Atlantic thermohaline circulation. *Geophys. Res. Lett.* **30**, doi:10.1029/2002GL015513 (2003).
29. Kawamura, K. *et al.* Northern Hemisphere forcing of climatic cycles in Antarctica over the past 360,000 years. *Nature* **448**, 912–917 (2007).
30. Huybers, P. Early Pleistocene glacial cycles and the integrated summer insolation forcing. *Science* **313**, 508–511 (2006).

Supplementary Information is linked to the online version of the paper at www.nature.com/nature.

Acknowledgements We thank T. Herbert, D. Oppo, Z. Liu, P. Huybers, A. Carlson and L. Robinson for discussions. L.E.L. was supported by the NOAA Postdoctoral Program in Climate and Global Change, administered by the University Corporation for Atmospheric Research. M.E.R. and W.B.C. acknowledge the support of NSF grants.

Author Contributions L.E.L. designed the study, performed the spectral analysis, and wrote the paper in consultation with M.E.R. and W.B.C.; contributed unpublished data from ODP Sites 926 and 928.

Author Information Reprints and permissions information is available at www.nature.com/reprints. Correspondence and requests for materials should be addressed to L.E.L. (lisiecki@alumni.brown.edu).